Published in final edited form as:
Cancer Res. 2012 May 15; 72(10): 2457–2467. doi:10.1158/0008-5472.CAN-11-2612.

A comprehensive survey of Ras mutations in cancer

Ian A. Prior[1,*], **Paul D. Lewis**[2], and **Carla Mattos**[3]

[1]Physiological Laboratory, Dept. of Molecular and Cellular Physiology, Institute of Translational Research, University of Liverpool, Liverpool, L69 3BX, UK.

[2]Cancer Informatics Group, Institute of Life Science, Swansea University, Swansea, SA2 8PP, UK. p.d.lewis@swansea.ac.uk Tel: +44-1792-295-222

[3]Department of Chemistry and Chemical Biology, Northeastern University, 102 Hurtig Hall, 360 Huntington Ave., Boston, MA 02115, USA c.mattos@neu.edu Tel: +1-617-373-2822

Abstract

All mammalian cells express three closely related Ras proteins: H-Ras, K-Ras and N-Ras that promote oncogenesis when mutationally activated at codons 12, 13 or 61. Despite a high degree of similarity between the isoforms, K-Ras mutations are far more frequently observed in cancer and each isoform displays preferential coupling to particular cancer types. We have examined the mutation spectra of Ras isoforms curated from large-scale tumour profiling and found that each isoform exhibits surprisingly distinctive codon mutation and amino acid substitution biases. These were unexpected given that these mutations occur in regions that share 100% amino acid sequence identity between the three isoforms. Importantly, many of the mutational biases were not due to differences in exposure to mutagens because the patterns were still evident when compared within specific cancer types. We discuss potential genetic and epigenetic mechanisms together with isoform-specific differences in protein structure and signalling that may promote these distinct mutation patterns and differential coupling to specific cancers.

Keywords

HRAS; KRAS; NRAS; GTPase; mutagenesis; mutation hotspot

Introduction

Ras proteins are proto-oncogenes that are frequently mutated in human cancers. They are encoded by three ubiquitously expressed genes: HRAS, KRAS and NRAS. These proteins are GTPases that function as molecular switches regulating pathways responsible for proliferation and cell survival. Ras proteins are normally tightly regulated by guanine nucleotide exchange factors (GEFs) promoting GDP dissociation and GTP binding and GTPase-activating proteins (GAPs) that stimulate the intrinsic GTPase activity of Ras to switch off signalling. Aberrant Ras function is associated with hyper-proliferative developmental disorders and cancer and in tumours is associated with a single mutation typically at codons 12, 13 or 61 (1). Mutation at these conserved sites favours GTP binding and produces constitutive activation of Ras (Figure 1). Importantly, all Ras isoforms share sequence identity in all of the regions responsible for GDP/GTP binding, GTPase activity, and effector interactions suggesting functional redundancy. Despite this, it has become increasingly apparent that Ras proteins exhibit isoform-specific functions (2). These

*Corresponding Author: iprior@liverpool.ac.uk Tel: +44-151-794-5332; Fax +44-151-794-4434 .

functional differences are most likely associated with the unique C-terminal hypervariable region (HVR) in each isoform, which is thought to modulate the Ras/membrane interaction to specify distinctive localizations in organelles and signalling nanoclusters (3).

An intriguing observation from the early days of Ras research was that different types of cancer appear to be coupled to mutation of a particular Ras isoform (4). We have revisited this unexplained phenomenon using latest data from large-scale collation of tumour sequencing to reveal additional patterns of isoform-specific codon and point mutation bias. We discuss the effects of these mutations on Ras function together with potential mechanisms leading to differential patterns of Ras isoform mutations.

Ras mutation frequencies

Large-scale tumour profiling

Early analysis of Ras isoform mutational status in cancer revealed varying incidences of Ras mutations in different tumour types and specific association of individual Ras isoforms with particular cancers (4). Despite relatively low sample sizes strong trends were identified, for example that K-Ras is the most frequently mutated isoform in most cancers with the extreme example of pancreatic cancer where 90% of tumours harboured K-Ras mutations. In contrast N-Ras mutations were more strongly associated with haematopoeitic tumours. The advent of large-scale tumour profiling and data sequencing databases now enables deeper analysis of Ras mutational spectra that was not possible with the limited sampling associated with previous studies. The catalogue of somatic mutations in cancer (COSMIC) represents the most comprehensive database on human tumour mutations currently available (5).

The COSMIC dataset confirms that K-Ras is the most frequently mutated isoform present in 22% of all tumours analysed compared to 8% for N-Ras and 3% for H-Ras (Table 1). These headline values indicate an often quoted compound mutation rate of 30%; however this is distorted by the screening bias evident within the dataset, particularly for K-Ras where colorectal cancer dominates the data totals. When all cancers where at least 20 tumours were counted are given equal weighting then the average pan-Ras mutation incidence is 16%.

With the exception of the salivary gland, screening has already been focussed on the locations and isoforms with the strongest coupling. Notably however, the pancreas mutation rate is 60% rather than the generally quoted 90%. In most cases one isoform dominates the number of mutations scored for a particular cancer. Thyroid, however, is an exception where large numbers of mutants of all three isoforms have been counted. While these observations confirm known trends, comparison of the codon mutations between the Ras isoforms reveals some intriguing deeper patterns.

Codon specificity of Ras isoform mutations

Analogous to the isoform bias we can see in specific cancers, analysis of codon mutation frequencies reveals that each isoform has a distinctive codon mutation signature (Figure 2). K-Ras and N-Ras represent two extremes of this phenomenon. 80% of K-Ras mutations occur at codon 12 whereas very few mutations are observed at codon 61. In contrast, almost 60% of N-Ras tumours harbour mutations at codon 61 versus 35% at codon 12. H-Ras displays an intermediate behaviour with an approximate 50%:40% split between mutations at codons 12 and 61 respectively. These data represent averages of percentages for each cancer where at least 20 tumours were scored. Importantly, closer examination of trends within different cancers confirms the individuality of each isoform even in circumstances where presumably the isoforms will have been exposed to common mutagenic factors (Figure 2B).

These differences in codon specificity are surprising because all three oncogenic mutations are in amino acid regions that are identical between the three isoforms and assumed to generate equivalent effects on protein activity. Notably, even at the DNA level K-Ras and N-Ras share identical sequences encoding Gly12 and Gln61. Furthermore, individual single base substitutions result in the same amino acid replacement for all of the isoforms. Despite this, examination of the preferred single base substitutions collated from all Ras mutated tumours in the COSMIC database reveals the final level of difference between the isoforms (Table 2).

Ras codons 12, 13 and 61 can each be converted to six other amino acids via single base substitutions. Despite this, >60% of the total mutations for each isoform are accounted for by only three of the 18 potential mutations across the codons (Table 2). K-Ras mutation patterns are dominated by the 43% that are G→A transitions at the second base of codons 12 or 13 resulting in G12D or G13D mutations. G→T transversions at the second base make up the bulk of the remainder to produce G12V although a special case exists in lung cancer where G→T transversion of the first base of codon 12 to produce G12C predominates. N-Ras favours similar types of mutations at codons 12 and 13 albeit at much lower rates than K-Ras. In contrast, H-Ras favours G12V in all cancers with codon 12 mutations and more generally exhibits a 3-fold higher proportion of transversion to transition mutations compared to K-Ras and N-Ras. Mutations at codon 61 recapitulate the heterogeneity evident between isoforms at codon 12.

These data reveal that Ras isoforms exhibit differential and preferential coupling to specific cancers, codons and substitutions generating oncogenic mutations. The distinct mutation patterns exhibited by Ras isoforms raise fundamental questions about their etiology. For example, do the mutation patterns reflect genetic or epigenetic differences between Ras isoforms that may lead to differential targetting of mutagens or repair processes? Additionally, how is this influenced by protein level effects such as relative Ras isoform abundance in tissues, cells and subcellular compartments or possibly isoform-specific differences in the effects of individual mutations on activity that combine to modulate signalling output and therefore relative oncogenicity?

Ras mutation etiology

Many genotoxic agents have been implicated in causing Ras mutations. Sequence motifs have been identified that correlate with highly reproducible mutagenesis. For example, classic chemical carcinogenesis studies showed that methylnitrosourea (MNU) targets the second base of codon 12 of H-Ras and K-Ras in a variety of cancer types to generate G12D mutations (6, 7). In contrast, UV-radiation targets pyrimidine dimers resulting in a high bias towards generating Ras Q61 mutations (8). The general trends in the dataset indicate predominantly bulky adduct induced damage for K-Ras mutations at codon 12 and chemical or UV-radiation induced damage for Q61 mutations in N-Ras.

It is clear that some of the observed mutational heterogeneity is due to tissue-specific exposure to different cocktails of mutagens. This is particularly the case when comparing mutation patterns across a single isoform. For example, lung cancer shows a highly distinctive coupling to G12C mutations (Table 2). The G.C→T.A transversions generating the G12C mutation have been associated in *in vitro* studies with bulky DNA adduct formation by tobacco smoke products (9). This specific mutation is most common in current smokers with incidence progressively declining to zero in former and never smokers (10). Whilst G12C appears to be a diagnostic mutation of exposure to tobacco smoke mutagens, it is far less abundant in pancreatic and colorectal cancers that are also strongly linked to smoking indicating tissue-specific differences in exposure to individual tobacco mutagens (11-13).

Other examples of potential tissue-specific mutagen exposure are colorectal cancer (CRC) and haematopoietic/lymphoid cancers where K-Ras and N-Ras exhibit unusually high preponderances of codon 13 mutations. Interestingly, in advanced CRC, G13D mutations have prognostic significance with anti-EGF receptor cetuximab-based therapy (14). This drug is not given to patients with K-Ras mutations because those with G12 mutations don't respond. However, patients with G13 mutated tumours showed significant improvements in survival indicating the importance of discriminating between Ras codon mutation types in designing clinical trials and treatment programmes.

Genetic and epigenetic influences

Some of the mutational bias implies differential exposure to mutagens. Whilst this may account for distinct mutations of K-Ras found in different cancers it doesn't explain why there is a difference between isoforms within the same cancer. The best example of this is thyroid carcinoma where significant numbers of mutations of all isoforms have been identified. This type of cancer has been particularly linked to exposure to ionising radiation as well as various chemical carcinogens (15). Comparison of mutation patterns across the Ras isoforms reveals clear bias with 95% of N-Ras mutations occurring at codon 61 whereas 66% of K-Ras mutations occur at codon 12. Analogous to the headline trends seen across all cancers, H-Ras has an intermediate profile with a 40%:50% split between codon 12 and codon 61 respectively. Within the codons the mutation patterns are also distinctive, for example at codon 12 K-Ras is predominantly G12D mutated whereas H-Ras favours G12V.

There has been little experimental analysis of the potential reasons for these differences to date. We can however use the empirical data available and draw some inferences from a larger number of studies carried out using the TP53 gene. We can then speculate that the heterogeneity could be due variables such as DNA primary sequence, secondary-quaternary structural effects and the position of the Ras genes within the genome and the nucleus. Together these effects may improve or limit access of different mutagens or repair enzymes.

Importantly, Ras isoform-specific differences in rates of DNA damage and repair have been identified. Tang and colleagues measured both adduct formation and subsequent repair of Ras isoforms following exposure to various bulky carcinogens including benzo[a]pyrene diol epoxide (BPDE) (16). They showed that codon 12 was the preferred binding site for BPDE on K-Ras but that adduct levels were reduced at this site in N-Ras and H-Ras. Other carcinogens including N-acetoxy-2-acetylaminofluorene (NAAAF) that have different modes of binding to the target guanine recapitulated this pattern. Significantly, whilst genomic DNA retained this K-Ras codon 12 targeting specificity for DNA adducts, PCR products of the primary target sequences did not (17). This mirrors a discrepancy between the observable BPDE adduct sites in human TP53, which occur at common smoking-related mutation hotspots in lung cancer (18), and the BPDE-induced mutation distribution from the p53 yeast functional assay (19). The yeast assay comprises a shorter TP53 cDNA construct rather than the entire gene sequence meaning the tertiary DNA structure surrounding mutation hotspots will differ to that in genomic DNA. These observations suggest that the binding potential of a carcinogen to a target nucleotide in both K-Ras and TP53 does not just depend on very local sequence context but also distal sequence and higher DNA organisation or modification.

Large scale surrounding sequence context may be an important determinant in shaping the pattern of Ras gene mutations. Whereas the amino acid sequence encoded by each isoform is almost identical across many species, the DNA sequence has considerable variation. Exon 1 sequence variation between isoforms could lead to differential formation of secondary structures such as hairpin loops during transcription. Examples of this are seen at common TP53 mutation hotspots correlated with a number of predicted stem-loop structures which

suggest that hypermutable bases frequently lie within single stranded DNA in close proximity to stems (20). In acute myeloid leukaemia (AML), K-Ras and N-Ras present a similar distribution of G.C→A.T and G.C→T.A mutations at codons 12. However, analysis of the COSMIC database reveals that the observable rate of mutations is almost six times greater for N-Ras compared to K-Ras. The expression level of N-Ras has been shown to be elevated relative to K-Ras in AML (21). Assuming a similar etiology for these mutations in either isoform it is possible that secondary structures formed during increased transcription lead to the higher mutation rate observed for N-Ras in AML tumours. Furthermore, the interplay between the target specificity of a particular mutagen and transcription-associated local secondary structure could explain the high levels of mutations at codon 12 relative to codon 61 in N-Ras which is rarely seen in other tumours. Surprisingly, a straightforward analysis of secondary structures has not been performed for codons 12, 13 and 61 in any Ras isoform to date.

Differences in DNA sequence between the Ras isoforms may also influence the repair efficiency of carcinogen adducts. Evidence for this comes from Tang and co-workers who found that repair of BPDE adducts at codon 12 of K-Ras was slower and thus inefficient compared to H-Ras and N-Ras (16). In TP53 it was found that BPDE adducts at major mutation hotspot positions are also regions of slow repair relative to other adduct sites (22). Furthermore, a number of these BPDE adduct sites are associated with low DNA curvature which is sequence dependent (23). Thus, local and more distal sequence context differences in Ras isoforms could result in differences in tertiary structure that significantly influence repair efficiencies.

The collective data provides evidence that increased adduct targetting and relatively poor repair renders K-Ras codon 12 far more likely to end up mutated and provides a plausible explanation for the higher K-Ras mutation rates observed in cancers. The reasons proposed for these differences in targetting and repair remain speculative. However, it is clear that the three Ras genes represent an excellent comparative model system for future investigation of the underlying genetic or epigenetic mechanisms leading to mutational spectra and hotspots.

Protein-based mechanisms

Structural implications of point mutations

The catalytic domain of Ras proteins consists of two lobes with an interface that includes switch II on the N-terminal lobe (residues 1-86) and helix 3 on the C-terminal lobe (residues 87-171) (24) (Figure 3A). The first can be thought of as the effector lobe, as it contains all of the Ras components that interact with effectors. The second is the allosteric lobe that interacts with the membrane (25) and contains all of the isoform specific differences outside of the HVR (24). Ras activation in response to the loading of GTP involves large conformational changes in switch I and switch II (26) as well as reorientation with respect to the membrane (27) that promote binding of effector proteins. Given the slow intrinsic hydrolysis rate measured in vitro for Ras (28), the deactivation of the signal is critically dependent on enhancement of GTPase activity by GAP (29) or by another mechanism such as the recently discovered allosteric switch associated with the RAS/RAF/MEK/ERK pathway (Figure 3B) (30, 31). In the latter case, a shift in helix 3/loop7 away from switch II is associated with a disorder to order transition that brings the catalytic Q61 residue into the active site upon binding of an acidic group, most likely a membrane component, at a remote allosteric site (30). The impaired ability of Ras mutants to hydrolyse GTP, either intrinsically or in response to GAPs, is responsible for the oncogenic nature of mutations at residues G12, G13 and Q61 in the active site. It is therefore important to understand the critical roles these residues play in facilitating catalysis.

The structure of Ras in complex with GAP solved in the presence of GDP and AlF_3 mimics the transition state of the hydrolysis reaction, with AlF_3 taking the place of the γ-phosphate in its planar conformation with the nucleophilic water molecule on one side and the GDP leaving group on the other (32). A prominent feature of this structure is the so-called GAP arginine finger that inserts into the RAS active site, providing a positive charge to stabilize negative charges that accumulate during the course of the hydrolysis reaction (Figure 3C) (33). The arginine finger is positioned in close van der Waals contact with the Cα atom of G12; this interaction would be displaced by any side chain at this position. Thus, mutants at G12 do not form the transition state complex with GAPs (34). As exemplified by G12D and G12P (35) as well as by G12V (34) they bind GAP with varying affinities with no increase in hydrolysis rates. Interestingly G12P is the only mutant of G12 that is non-transforming in cells (36), does not appear in any tumours (Table 2) and has a normal or slightly enhanced intrinsic hydrolysis rate (35). Although not much can be found in the literature on the structural biology of mutations at G13, it is clear from the Ras/RasGAP structure that any side chain at this position would also clash to some extent with the arginine finger in GAP. Consistently, small side chains at this position, such as G13A and G13V are able to form the transition state complex with GAP, but larger ones such as G13R cannot (34).

In addition to contributing a catalytic residue, GAP enhances the hydrolysis rate by ordering switch II and placing Q61 in the active site. In doing so it also promotes a shift in helix 3/loop 7 similar to that described above for the allosteric switch. The amide group of the Q61 side chain H-bonds to the carbonyl group of the GAP arginine finger, helping to position it in the active site, while its side chain carbonyl group accepts an H-bond from the nucleophilic water molecule. Glutamine is the only one of the 20 amino acid residues that could serve this dual function, since asparagine would not reach far enough into the active site. Thus, while a mutant such as Q61L does bind GAP with affinity similar to that of wild type (37) it cannot form the transition state mimic (34) and its hydrolysis rate is not enhanced by the interaction (38).

The Ras active site conformation associated with intrinsic hydrolysis is also impaired by the oncogenic mutants at positions 12, 13 and 61 (31) (Figure 3D). In intrinsic hydrolysis in the presence of Raf, where switch II is proposed to be ordered through the allosteric switch mechanism, the conserved switch I residue Y32 partially overlaps with the position where the GAP arginine finger would bind and its hydroxyl group is bridged to the γ-phosphate of GTP through a second catalytic water molecule, the bridging water, that also interacts with catalytic residue Q61 (30). Although a structure mimicking the transition state of this reaction is not yet available, it is proposed that during activation of the nucleophilic water a proton is shuttled through the γ-phosphate to the bridging water molecule, providing a partial positive charge that stabilizes negative charges developed during the reaction in lieu of the GAP arginine finger (30). Mutations at G12 and Q61 have similar effects by displacing the bridging water molecule and disallowing the positioning of residue 61 as seen in the wild type (31) (Figure 3D). The structure of G12D shows similar perturbations in the active site, but this time one of its side chain carboxyl groups takes the place of the bridging water in connecting Y32 to the γ-phosphate of GTP, while its other side chain oxygen atom H-bonds to the Q61 side chain (35) (Figure 3D). All mutants of either G12 (except for G12P) or Q61 result in at least a 10-fold decrease in intrinsic hydrolysis rate measured in vitro. Unfortunately very little biochemical and structural information is available for the G13 mutants, but it is clear that any side chain at this position would clash with the position of Y32 in the active site conformation associated with intrinsic hydrolysis.

It is clear from the Ras mutation spectra in Table 2 that G12D, G12V, Q61K, Q61L and Q61R mutations predominate over others. However, although the structural perturbations of the active site caused by these mutants explain how they may contribute to oncogenic

transformation, they do not explain their prevalence over other mutants such as G12I or Q61V that are expected to have similar active site perturbations and are equally potent in promoting transformation in NIH-3T3 cells (36, 39). In vitro experiments indicated that the most highly transforming G12 mutants in cells are I, V, L, T and R (36). G12I/L/T mutations require more than one base substitution to occur explaining their relative rarity; in contrast, the highly potent G12R requires a single substitution of the first base yet is also rare. It is notable that the most frequently observed mutations, G12D and G12V, occur following middle base substitutions. Whilst there is no obvious protein structural reason for their predominance we speculate that their abundance may reflect their relative potency combined with a broad specificity of mutagens for the changing the middle base of codon 12.

The situation is much more clear for the Q61 mutants, where V, L, K, A, C and R are the most highly transforming mutants in NIH-3T3 cells (39). Of these, only L, K and R, the most predominant Q61 mutants, result from single base changes in the wild type codon for glutamine. The structural origin for the potency of the Q61 highly transforming mutants is that in addition to perturbing the conformation of the active site associated catalysis as described above, these mutants shift the conformational equilibrium toward an anticatalytic conformation of switch II when in the complex with RAF (40).

Since the effector lobe is identical in all isoforms, the isoform specific preferences for G12, G13 or Q61 mutations shown in Figure 2 must be due to components that interact with the membrane, entirely found in the allosteric lobe (Figure 3A) and the C-terminal HVR. The HVR in particular carries low homology between the isoforms and directs localization in membrane environments with distinct composition for each isoform (3). Interaction at the recently discovered allosteric site may be sensitive to the membrane composition and this site is directly linked to the active site through the allosteric switch, which in turn may be affected differently by the various oncogenic mutations.

Isoform-specific Ras signalling

A final contribution to generating the bias in Ras mutation frequencies could be distinctive signal outputs by Ras isoforms. Despite being almost identical they are not functionally redundant. The main current model for explaining isoform-specific Ras signalling involves compartmentalization (3, 41, 42). This is based on the fact that the only area of significant protein sequence divergence between the isoforms is in the final 25/26 amino acid HVR that contains all of the membrane binding and trafficking information (Figure 1). Whilst the plasma membrane is the major location for all Ras isoforms they have also been localized to intracellular membranes including the ER, Golgi, endosomal network and mitochondria (2). Each isoform is present in these locations in different concentrations due to differences in total abundance, specific targetting and relative affinity (43-49). These differences in relative localization are believed to enable the Ras isoforms to come into contact with different pools of regulators and effectors to generate overlapping but distinctive outputs.

Over 20 effectors have been identified that can be broadly categorised as kinases or regulators of other GTPases (2). The most important are the proliferation inducing Raf-MEK-ERK kinase cascade and the phosphatidylinositol 3-kinase (PI3K)-protein kinase B (PKB)/Akt pathway that promotes cell survival. *In vitro* experiments have shown that H-Ras is a better activator of PI3K whereas K-Ras is more strongly coupled to Raf and Rac (50-52). Of more significance, endogenous isoform-specific differences have been identified in human and mouse development. In humans, germ-line mutations of each isoform generates overlapping but distinctive sets of neuro-cardio-facial proliferative disorders (53). These mutations also favour Ras activation but are largely distinct from the main oncogenic mutations (Figure 1). In mice, K-Ras knockout is lethal whereas N-Ras and H-Ras double

knockout mice develop apparently normally (54-56). Importantly, H-Ras is able to substitute for K-Ras when placed under the same endogenous locus (57). Together, this indicates that precisely co-ordinated expression is critical and argues against pathways uniquely regulated by individual isoforms.

Whilst all isoforms have been investigated for their oncogenic signalling properties there have been relatively few studies where all three have been directly compared. A good *in vitro* model for future work is the isogenic cell approach where mutant endogenous genes can be compared in an identical genetic background. Using this type of approach, K-Ras was shown to be more potent at generating colorectal cell transformation and modulating signalling compared to the other isoforms (58). Equivalent mouse models with oncogenic mutations to endogenous genes have also been instructive. In genetically engineered mice, G12D mutated K-Ras but not N-Ras promoted widespread colonic epithelial hyperplasia and also neoplasia when in combination with APC mutations commonly seen in colon cancer (59). The unique capacity of K-Ras to promote colorectal adenocarcinoma was proposed to link to proliferative pathway signalling via Raf; in contrast, N-Ras triggered cell survival pathways to inhibit apoptosis (59, 60). Interestingly, mutant N-Ras but not K-Ras conferred resistance to apoptosis in response to the inflammatory cytokine TNFα; suggesting a model where the relatively infrequent N-Ras mutations associated with colorectal cancer may be associated with selective pressure exerted by chronic inflammation (60, 61).

The data on isoform-specific signalling are not yet comprehensive however it seems clear that the differences are relatively subtle and tissue context specific. This is exemplified in comparative studies that revealed that G12V mutated K-Ras promotes endodermal stem cell expansion by promoting proliferation and inhibiting differentiation (62). In contrast, mutant N-Ras had no detectable effect whilst H-Ras G12V actively promoted differentiation. All Ras isoforms differentially used the same effector pathways to achieve these disparate effects (62). These results are significant because many cancers including pancreas, lung and colorectal are of endodermal origin. These data suggest a model where K-Ras coupling to these major cancer types is via its role in expanding cancer progenitor cells in these tissues (1, 63).

It is important to note that signalling will also be highly context dependent. The beneficial effects of G13D versus G12D mutations as prognostic indicators for anti-EGFR therapy in advanced CRC are not evident in non-small cell lung cancer (NSCLC) (14, 64). A parallel observation is that the Ras effectors, BRAF and PIK3CA are far more frequently mutated in CRC (11-13%) compared to NSCLC (1-2%) and pancreatic carcinoma (<1%). This implies different dependency on activation of specific effector pathways in cancer types exhibiting high rates of KRAS mutations (17-61%) and suggests differential coupling between KRAS and key effector pathways. Based on the G12D/G13D observations in advanced CRC it is also tempting to speculate that specific cancers may be promoted predominantly by upregulation of particular signalling pathways that may be most sensitive to mutations at a given residue. Strong support for this notion comes from work on the Ras allosteric switch associated specifically with the Ras/RAF/MEK/ERK pathway where the Ras/RAF interaction severely impairs hydrolysis in highly transforming Q61 mutants such as Q61L and Q61K (40). Thus the Q61 mutants are expected to have a very strong oncogenic effect where the RAF pathway is primarily involved in promoting the cancer through misfunction of the allosteric switch. Interestingly N-Ras, for which Q61 mutants are particularly prominent in cancers is also the only isoform for which a mutation in the allosteric site has been found in tumours (at the R97 position, Figure 1).

In summary, these data reveal that Ras isoforms are differentially capable of influencing important phenotypic responses that contribute to cancer initiation and progression. K-Ras

appears to be the most capable of sustaining cancer programmes and this would translate into strong selective pressure for mutations of this isoform. However, it is striking that despite a prolonged period of investigation, that the differences in signal network responses responsible for the pre-eminence of K-Ras over the other isoforms and their context dependent signalling remain largely uncharacterised.

Conclusions

We have identified differences in mutational spectra between the three Ras isoforms that are likely to be a consequence of multiple interacting intrinsic and extrinsic factors. Tissue-specific comparison between isoforms indicates that these are not simply due to differences in mutagen exposure that could create the heterogeneity observed across a single isoform. We have identified genetic, epigenetic and protein based mechanisms that may contribute to generating these mutational spectra. The expression of three almost identical Ras isoforms from separate gene loci presents a unique opportunity to deconvolve the effects. Consequently, they represent the ideal model system for probing generic questions about mutagenesis, carcinogenesis, signalling network integration and how contextual influences such as relative abundance, tissue expression and subcellular localization modulate these complex phenomena. We anticipate important advances in our understanding of these areas in the near future with the development of large scale screening platforms, isogenic model systems and a more systematic approach to analysing the isoforms in parallel.

Acknowledgments

IAP is a Royal Society University Research Fellow, research in his laboratory is funded by the Wellcome Trust, NWCRF and BBSRC. PDL receives funding from the National Institute for Social Care and Health Research and Welsh Government. Ras research in the Mattos laboratory is funded by the NIH grant R56-CA096867. Thanks to Greg Buhrman for making Figure 3.

References

1. Quinlan MP, Settleman J. Isoform-specific ras functions in development and cancer. Future Oncol. 2009; 5(1):105–16. [PubMed: 19243303]
2. Omerovic J, Laude AJ, Prior IA. Ras proteins: paradigms for compartmentalised and isoform-specific signalling. Cell Mol Life Sci. 2007; 64(19-20):2575–89. [PubMed: 17628742]
3. Henis YI, Hancock JF, Prior IA. Ras acylation, compartmentalization and signaling nanoclusters (Review). Mol Membr Biol. 2009; 26(1):80–92. [PubMed: 19115142]
4. Bos JL. ras oncogenes in human cancer: a review. Cancer Res. 1989; 49(17):4682–9. [PubMed: 2547513]
5. Forbes SA, Bindal N, Bamford S, Cole C, Kok CY, Beare D, et al. COSMIC: mining complete cancer genomes in the Catalogue of Somatic Mutations in Cancer. Nucleic Acids Res. 2011; 39(Database issue):D945–50. [PubMed: 20952405]
6. Zarbl H, Sukumar S, Arthur AV, Martin-Zanca D, Barbacid M. Direct mutagenesis of Ha-ras-1 oncogenes by N-nitroso-N-methylurea during initiation of mammary carcinogenesis in rats. Nature. 1985; 315(6018):382–5. [PubMed: 3923365]
7. Barbacid M. ras oncogenes: their role in neoplasia. Eur J Clin Invest. 1990; 20(3):225–35. [PubMed: 2114981]
8. Tormanen VT, Pfeifer GP. Mapping of UV photoproducts within ras proto-oncogenes in UV-irradiated cells: correlation with mutations in human skin cancer. Oncogene. 1992; 7(9):1729–36. [PubMed: 1501884]
9. Seo KY, Jelinsky SA, Loechler EL. Factors that influence the mutagenic patterns of DNA adducts from chemical carcinogens. Mutat Res. 2000; 463(3):215–46. [PubMed: 11018743]

10. Le Calvez F, Mukeria A, Hunt JD, Kelm O, Hung RJ, Taniere P, et al. TP53 and KRAS mutation load and types in lung cancers in relation to tobacco smoke: distinct patterns in never, former, and current smokers. Cancer Res. 2005; 65(12):5076–83. [PubMed: 15958551]
11. Hecht SS. Tobacco carcinogens, their biomarkers and tobacco-induced cancer. Nat Rev Cancer. 2003; 3(10):733–44. [PubMed: 14570033]
12. Porta M, Crous-Bou M, Wark PA, Vineis P, Real FX, Malats N, et al. Cigarette smoking and K-ras mutations in pancreas, lung and colorectal adenocarcinomas: etiopathogenic similarities, differences and paradoxes. Mutat Res. 2009; 682(2-3):83–93. [PubMed: 19651236]
13. Capella G, Cronauer-Mitra S, Pienado MA, Perucho M. Frequency and spectrum of mutations at codons 12 and 13 of the c-K-ras gene in human tumors. Environ Health Perspect. 1991; 93:125–31. [PubMed: 1685441]
14. De Roock W, Jonker DJ, Di Nicolantonio F, Sartore-Bianchi A, Tu D, Siena S, et al. Association of KRAS p.G13D mutation with outcome in patients with chemotherapy-refractory metastatic colorectal cancer treated with cetuximab. Jama. 2010; 304(16):1812–20. [PubMed: 20978259]
15. Sipos JA, Mazzaferri EL. Thyroid cancer epidemiology and prognostic variables. Clin Oncol (R Coll Radiol). 22(6):395–404. [PubMed: 20627675]
16. Feng Z, Hu W, Chen JX, Pao A, Li H, Rom W, et al. Preferential DNA damage and poor repair determine ras gene mutational hotspot in human cancer. J Natl Cancer Inst. 2002; 94(20):1527–36. [PubMed: 12381705]
17. Hu W, Feng Z, Tang MS. Preferential carcinogen-DNA adduct formation at codons 12 and 14 in the human K-ras gene and their possible mechanisms. Biochemistry. 2003; 42(33):10012–23. [PubMed: 12924950]
18. Denissenko MF, Pao A, Tang M, Pfeifer GP. Preferential formation of benzo[a]pyrene adducts at lung cancer mutational hotspots in P53. Science. 1996; 274(5286):430–2. [PubMed: 8832894]
19. Yoon JH, Lee CS, Pfeifer GP. Simulated sunlight and benzo[a]pyrene diol epoxide induced mutagenesis in the human p53 gene evaluated by the yeast functional assay: lack of correspondence to tumor mutation spectra. Carcinogenesis. 2003; 24(1):113–9. [PubMed: 12538356]
20. Wright BE, Reimers JM, Schmidt KH, Reschke DK. Hypermutable bases in the p53 cancer gene are at vulnerable positions in DNA secondary structures. Cancer Res. 2002; 62(20):5641–4. [PubMed: 12384517]
21. Gougopoulou DM, Kiaris H, Ergazaki M, Anagnostopoulos NI, Grigoraki V, Spandidos DA. Mutations and expression of the ras family genes in leukemias. Stem Cells. 1996; 14(6):725–9. [PubMed: 8948029]
22. Denissenko MF, Pao A, Pfeifer GP, Tang M. Slow repair of bulky DNA adducts along the nontranscribed strand of the human p53 gene may explain the strand bias of transversion mutations in cancers. Oncogene. 1998; 16(10):1241–7. [PubMed: 9546425]
23. Lewis PD, Parry JM. In silico p53 mutation hotspots in lung cancer. Carcinogenesis. 2004; 25(7): 1099–107. [PubMed: 14729588]
24. Gorfe AA, Grant BJ, McCammon JA. Mapping the nucleotide and isoform-dependent structural and dynamical features of Ras proteins. Structure. 2008; 16(6):885–96. [PubMed: 18547521]
25. Gorfe AA, Hanzal-Bayer M, Abankwa D, Hancock JF, McCammon JA. Structure and dynamics of the full-length lipid-modified H-Ras protein in a 1,2-dimyristoylglycero-3-phosphocholine bilayer. J Med Chem. 2007; 50(4):674–84. [PubMed: 17263520]
26. Vetter IR, Wittinghofer A. The guanine nucleotide-binding switch in three dimensions. Science. 2001; 294(5545):1299–304. [PubMed: 11701921]
27. Abankwa D, Gorfe AA, Hancock JF. Mechanisms of Ras membrane organization and signalling: Ras on a rocker. Cell Cycle. 2008; 7(17):2667–73. [PubMed: 18758236]
28. John J, Schlichting I, Schiltz E, Rosch P, Wittinghofer A. C-terminal truncation of p21H preserves crucial kinetic and structural properties. J Biol Chem. 1989; 264(22):13086–92. [PubMed: 2502546]
29. Ahmadian MR, Wiesmuller L, Lautwein A, Bischoff FR, Wittinghofer A. Structural differences in the minimal catalytic domains of the GTPase-activating proteins p120GAP and neurofibromin. J Biol Chem. 1996; 271(27):16409–15. [PubMed: 8663212]

30. Buhrman G, Holzapfel G, Fetics S, Mattos C. Allosteric modulation of Ras positions Q61 for a direct role in catalysis. Proc Natl Acad Sci U S A. 2010; 107(11):4931–6. [PubMed: 20194776]
31. Buhrman G, Kumar VS, Cirit M, Haugh JM, Mattos C. Allosteric modulation of Ras-GTP is linked to signal transduction through RAF kinase. J Biol Chem. 2011; 286(5):3323–31. [PubMed: 21098031]
32. Scheffzek K, Ahmadian MR, Kabsch W, Wiesmuller L, Lautwein A, Schmitz F, et al. The Ras-RasGAP complex: structural basis for GTPase activation and its loss in oncogenic Ras mutants. Science. 1997; 277(5324):333–8. [PubMed: 9219684]
33. Maegley KA, Admiraal SJ, Herschlag D. Ras-catalyzed hydrolysis of GTP: a new perspective from model studies. Proc Natl Acad Sci U S A. 1996; 93(16):8160–6. [PubMed: 8710841]
34. Gremer L, Gilsbach B, Ahmadian MR, Wittinghofer A. Fluoride complexes of oncogenic Ras mutants to study the Ras-RasGap interaction. Biol Chem. 2008; 389(9):1163–71. [PubMed: 18713003]
35. Franken SM, Scheidig AJ, Krengel U, Rensland H, Lautwein A, Geyer M, et al. Three-dimensional structures and properties of a transforming and a nontransforming glycine-12 mutant of p21H-ras. Biochemistry. 1993; 32(33):8411–20. [PubMed: 8357792]
36. Seeburg PH, Colby WW, Capon DJ, Goeddel DV, Levinson AD. Biological properties of human c-Ha-ras1 genes mutated at codon 12. Nature. 1984; 312(5989):71–5. [PubMed: 6092966]
37. Vogel US, Dixon RA, Schaber MD, Diehl RE, Marshall MS, Scolnick EM, et al. Cloning of bovine GAP and its interaction with oncogenic ras p21. Nature. 1988; 335(6185):90–3. [PubMed: 2842690]
38. Gibbs JB, Schaber MD, Allard WJ, Sigal IS, Scolnick EM. Purification of ras GTPase activating protein from bovine brain. Proc Natl Acad Sci U S A. 1988; 85(14):5026–30. [PubMed: 3293047]
39. Der CJ, Finkel T, Cooper GM. Biological and biochemical properties of human rasH genes mutated at codon 61. Cell. 1986; 44(1):167–76. [PubMed: 3510078]
40. Buhrman G, Wink G, Mattos C. Transformation efficiency of RasQ61 mutants linked to structural features of the switch regions in the presence of Raf. Structure. 2007; 15(12):1618–29. [PubMed: 18073111]
41. Mor A, Philips MR. Compartmentalized Ras/MAPK signaling. Annu Rev Immunol. 2006; 24:771–800. [PubMed: 16551266]
42. Rocks O, Peyker A, Bastiaens PI. Spatio-temporal segregation of Ras signals: one ship, three anchors, many harbors. Curr Opin Cell Biol. 2006; 18(4):351–7. [PubMed: 16781855]
43. Apolloni A, Prior IA, Lindsay M, Parton RG, Hancock JF. H-ras but not K-ras traffics to the plasma membrane through the exocytic pathway. Mol Cell Biol. 2000; 20(7):2475–87. [PubMed: 10713171]
44. Bivona TG, Quatela SE, Bodemann BO, Ahearn IM, Soskis MJ, Mor A, et al. PKC regulates a farnesyl-electrostatic switch on K-Ras that promotes its association with Bcl-XL on mitochondria and induces apoptosis. Mol Cell. 2006; 21(4):481–93. [PubMed: 16483930]
45. Choy E, Chiu VK, Silletti J, Feoktistov M, Morimoto T, Michaelson D, et al. Endomembrane trafficking of ras: the CAAX motif targets proteins to the ER and Golgi. Cell. 1999; 98(1):69–80. [PubMed: 10412982]
46. Rocks O, Gerauer M, Vartak N, Koch S, Huang ZP, Pechlivanis M, et al. The palmitoylation machinery is a spatially organizing system for peripheral membrane proteins. Cell. 2010; 141(3): 458–71. [PubMed: 20416930]
47. Roy S, Wyse B, Hancock JF. H-Ras signaling and K-Ras signaling are differentially dependent on endocytosis. Mol Cell Biol. 2002; 22(14):5128–40. [PubMed: 12077341]
48. Jura N, Scotto-Lavino E, Sobczyk A, Bar-Sagi D. Differential modification of Ras proteins by ubiquitination. Mol Cell. 2006; 21(5):679–87. [PubMed: 16507365]
49. Prior IA, Muncke C, Parton RG, Hancock JF. Direct visualization of Ras proteins in spatially distinct cell surface microdomains. J Cell Biol. 2003; 160(2):165–70. [PubMed: 12527752]
50. Walsh AB, Bar-Sagi D. Differential activation of the Rac pathway by Ha-Ras and K-Ras. J Biol Chem. 2001; 276(19):15609–15. [PubMed: 11278702]
51. Yan J, Roy S, Apolloni A, Lane A, Hancock JF. Ras isoforms vary in their ability to activate Raf-1 and phosphoinositide 3-kinase. J Biol Chem. 1998; 273(37):24052–6. [PubMed: 9727023]

52. Voice JK, Klemke RL, Le A, Jackson JH. Four human ras homologs differ in their abilities to activate Raf-1, induce transformation, and stimulate cell motility. J Biol Chem. 1999; 274(24): 17164–70. [PubMed: 10358073]
53. Tidyman WE, Rauen KA. The RASopathies: developmental syndromes of Ras/MAPK pathway dysregulation. Curr Opin Genet Dev. 2009; 19(3):230–6. [PubMed: 19467855]
54. Esteban LM, Vicario-Abejon C, Fernandez-Salguero P, Fernandez-Medarde A, Swaminathan N, Yienger K, et al. Targeted genomic disruption of H-ras and N-ras, individually or in combination, reveals the dispensability of both loci for mouse growth and development. Mol Cell Biol. 2001; 21(5):1444–52. [PubMed: 11238881]
55. Koera K, Nakamura K, Nakao K, Miyoshi J, Toyoshima K, Hatta T, et al. K-ras is essential for the development of the mouse embryo. Oncogene. 1997; 15(10):1151–9. [PubMed: 9294608]
56. Umanoff H, Edelmann W, Pellicer A, Kucherlapati R. The murine N-ras gene is not essential for growth and development. Proc Natl Acad Sci U S A. 1995; 92(5):1709–13. [PubMed: 7878045]
57. Potenza N, Vecchione C, Notte A, De Rienzo A, Rosica A, Bauer L, et al. Replacement of K-Ras with H-Ras supports normal embryonic development despite inducing cardiovascular pathology in adult mice. EMBO Rep. 2005; 6(5):432–7. [PubMed: 15864294]
58. Keller JW, Franklin JL, Graves-Deal R, Friedman DB, Whitwell CW, Coffey RJ. Oncogenic KRAS provides a uniquely powerful and variable oncogenic contribution among RAS family members in the colonic epithelium. J Cell Physiol. 2007; 210(3):740–9. [PubMed: 17133351]
59. Haigis KM, Kendall KR, Wang Y, Cheung A, Haigis MC, Glickman JN, et al. Differential effects of oncogenic K-Ras and N-Ras on proliferation, differentiation and tumor progression in the colon. Nat Genet. 2008; 40(5):600–8. [PubMed: 18372904]
60. Kreeger PK, Wang Y, Haigis KM, Lauffenburger DA. Integration of multiple signaling pathway activities resolves K-RAS/N-RAS mutation paradox in colon epithelial cell response to inflammatory cytokine stimulation. Integr Biol (Camb). 2010; 2(4):202–8. [PubMed: 20473400]
61. Burmer GC, Levine DS, Kulander BG, Haggitt RC, Rubin CE, Rabinovitch PS. c-Ki-ras mutations in chronic ulcerative colitis and sporadic colon carcinoma. Gastroenterology. 1990; 99(2):416–20. [PubMed: 2194896]
62. Quinlan MP, Quatela SE, Philips MR, Settleman J. Activated Kras, but not Hras or Nras, may initiate tumors of endodermal origin via stem cell expansion. Mol Cell Biol. 2008; 28(8):2659–74. [PubMed: 18268007]
63. Quinlan MP, Settleman J. Explaining the preponderance of Kras mutations in human cancer: An isoform-specific function in stem cell expansion. Cell Cycle. 2008; 7(10):1332–5. [PubMed: 18418066]
64. O'Byrne KJ, Gatzemeier U, Bondarenko I, Barrios C, Eschbach C, Martens UM, et al. Molecular biomarkers in non-small-cell lung cancer: a retrospective analysis of data from the phase 3 FLEX study. Lancet Oncol. 2011
65. Cox AD, Der CJ. Ras history: The saga continues. Small Gtpases. 2011; 1(1):2–27. [PubMed: 21686117]
66. Goody RS, Pai EF, Schlichting I, Rensland H, Scheidig A, Franken S, et al. Studies on the structure and mechanism of H-ras p21. Philos Trans R Soc Lond B Biol Sci. 1992; 336(1276):3–10. discussion -1. [PubMed: 1351293]

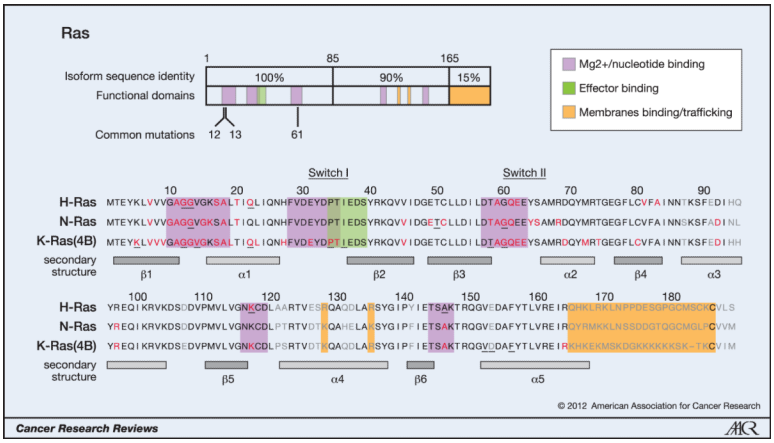

Figure 1. Oncogenic mutations of Ras isoforms

The key oncogenic mutations are in the region that is identical between the three isoforms. 44 separate point mutations have been characterised in Ras isoforms with 99.2% of all mutations occurring at codons 12, 13 and 61. Mutations cluster in and around loops 1, 2 and 4 responsible for nucleotide binding and result in enhanced GTP binding. Residues mutated in cancer are highlighted in red, those mutated in developmental disorders are underlined and residues that are variable between isoforms are in grey (26, 65, 66).

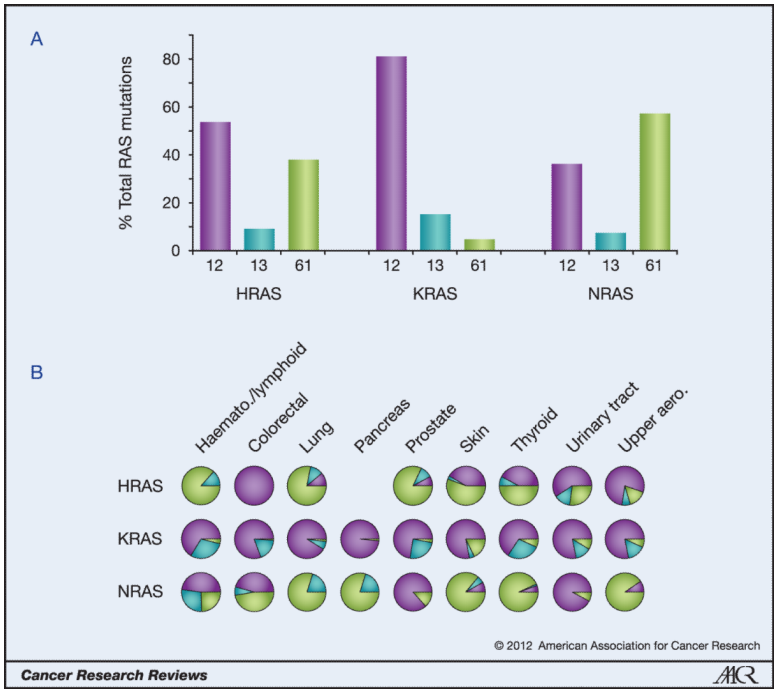

Figure 2. Ras isoform-specific codon mutation bias

A. K-Ras is typically mutated at codon 12 whereas N-Ras favours codon 61. H-Ras displays intermediate behaviour. Data are averages of percentages collated from all cancers with at least 20 tumours scored. B. Analysis of individual cancer types reveals isoform-specific patterns of codon mutation even within the same tissue. Pie chart colours - black: codon 12; grey: codon 13; white: codon 61.

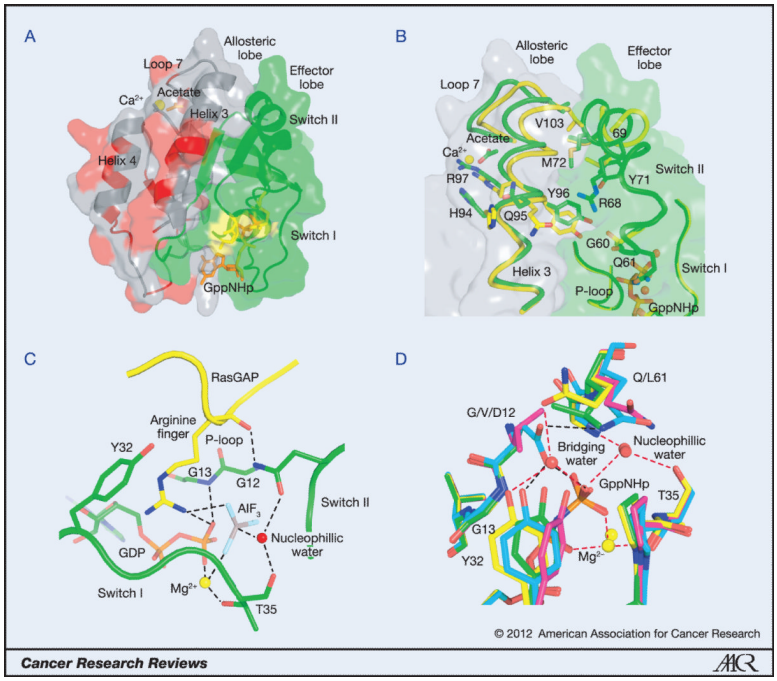

Figure 3. Structural features of Ras and its oncogenic mutations

A. The catalytic domain of Ras. The effector lobe is depicted in green and the allosteric lobe in grey. Residues that are not identical in all three isoforms are in red and are found entirely in the allosteric lobe. Residues 12, 13 and 61 are shown in yellow and GppNHp is in orange. Calcium acetate is shown bound at the allosteric site. B. The allosteric switch showing some of the key residues involved. The allosteric state in which switch II is disordered is shown in yellow (PDB code 2RGE). Residues 61-68 are disordered and therefore were removed from the model. The structure with calcium acetate in the allosteric site interacting with R97 is shown in green (PDB code 3K8Y). Switch II is ordered in this structure. The nucleotide is depicted in orange. C. The active site in the Ras/RasGAP complex (PDB code 1WQ1). GAP residues are shown in yellow with the arginine finger shown in stick. Ras residues are in green, including the GDP with phosphate groups in orange. AlF_3 is shown with the aluminum atom in grey and fluorine atoms in cyan. G12, G13, Y32 T35 and Q61 are shown in stick. The Mg^{2+} ion is depicted as a yellow sphere and the nucleophilic water molecule as a red sphere. D. The active site for intrinsic hydrolysis in Ras. The wild type is shown in yellow (PDB code 3K8Y), G12V in magenta (PDB code 3OIW), G12D in cyan (PDB code 1AGP) and Q61L in green (PDB code 3OIU). The wild type structure contains both the nucleophilic and bridging water molecules. Note that in G12D the side chain of D12 replaces the bridging water molecule, whereas in G12V and Q61L there is a direct H-bond between Y32 and the γ-phosphate of the nucleotide. Mg^{2+} is shown in yellow sphere and water molecules in red spheres in each structure. Hydrogen bonds in the wild type structure are depicted in red dashed lines. Those in the G12D mutant are in black dashed line. H-bonds in the G12V and Q61L structures are not shown. Note the proximity of G13 to the Y32 side chain in the wild type structure.

Cancer Res. Author manuscript; available in PMC 2012 November 15.

Table 1

Incidence of Ras isoform mutations in cancer

Most cancer types favour mutation of a single isoform; this is typically K-Ras. + is the number of tumours observed with this mutant Ras, n is the number of unique samples screened. Data collated from COSMIC v52 release.

	HRAS			KRAS			NRAS			Pan-Ras
Primary tissue	**+**	**n**	**%**	**+**	**n**	**%**	**+**	**n**	**%**	**%**
adrenal gland	1	135	<1%	1	210	<1%	7	170	4%	5%
autonomic ganglia	0	63	0%	2	63	3%	7	102	7%	10%
biliary tract	0	151	0%	460	1471	31%	3	213	1%	33%
bone	3	147	2%	2	165	1%	0	143	0%	3%
breast	5	542	<1%	20	544	4%	7	330	2%	7%
central nervous system	0	942	0%	8	1032	<1%	8	995	<1%	2%
cervix	23	264	9%	46	637	7%	2	132	2%	17%
endometrium	3	291	1%	298	2108	14%	1	279	<1%	16%
haematopoietic/lymphoid	8	3074	<1%	277	5757	5%	877	8540	10%	15%
kidney	1	273	<1%	4	617	<1%	2	435	<1%	1%
large intestine	2	617	<1%	9671	29183	33%	26	1056	3%	36%
liver	0	270	0%	21	450	5%	8	310	3%	7%
lung	9	1957	<1%	2533	14632	17%	26	2678	1%	19%
oesophagus	2	161	1%	13	359	4%	0	161	0%	5%
ovary	0	94	0%	406	2934	14%	5	111	5%	18%
pancreas	0	221	0%	3127	5169	61%	5	248	2%	63%
prostate	29	500	6%	82	1024	8%	8	530	2%	15%
salivary gland	24	161	15%	5	170	3%	0	45	0%	18%
skin	120	1940	6%	38	1405	3%	858	4742	18%	27%
small intestine	0	5	0%	62	316	20%	0	5	0%	20%
stomach	14	384	4%	163	2571	6%	5	215	2%	12%
testis	5	130	4%	17	432	4%	8	283	3%	11%
thymus	1	46	2%	4	186	2%	0	46	0%	4%
thyroid	117	3601	3%	137	4628	3%	312	4126	8%	14%
upper aerodigestive tract	101	1083	9%	52	1535	3%	24	807	3%	16%
urinary tract	138	1242	11%	29	591	5%	9	398	2%	18%

Primary tissue	HRAS +	HRAS n	HRAS %	KRAS +	KRAS n	KRAS %	NRAS +	NRAS n	NRAS %	Pan-Ras %
Total	606	18294	3%	17478	78189	22%	2208	27100	8%	16%

Table 2

Isoform-specific point mutation specificity

Data representing total numbers of tumours with each point mutation are collated from COSMIC v52 release. Single base mutations generating each amino acid substitution are indicated. The most frequent mutations for each isoform for each cancer type are highlighted with grey shading. H/L: Haematopoeitic/lymphoid tissues.

HRAS		codon 12: GGC						codon 13: GGT						codon 61: CAG						
		-C-	T--	-A-	C--	A--	-T-	-C-	T--	-A-	C--	A--	-T-	G--	--C/T	A--	-T-	-C-	-G-	
Primary tissue	cancer	12A	12C	12D	12R	12S	12V	13A	13C	13D	13R	13S	13V	61E	61H	61K	61L	61P	61R	Total
prostate	adenocarcinoma	0	0	0	0	1	1	0	0	0	3	0	0	0	3	0	18	0	3	29
salivary gland	adenocarcinoma	0	0	1	4	1	8	0	0	0	3	0	0	0	0	0	0	0	6	23
skin	benign melanocytic nevus	0	0	0	1	0	0	0	0	0	1	0	0	0	1	1	20	0	11	35
	carcinoma	0	2	2	0	0	24	0	0	1	0	0	0	0	3	0	3	0	0	35
	malignant melanoma	0	0	0	0	0	2	0	0	1	0	0	0	0	1	2	3	0	2	11
stomach	adenocarcinoma	0	0	0	0	0	14	0	0	0	0	0	0	0	0	0	0	0	0	14
thyroid	adenoma-nodule-goitre	0	0	0	0	0	19	0	0	0	0	0	0	0	1	4	0	1	16	41
	carcinoma	2	2	2	1	2	19	0	2	3	6	0	0	0	2	10	1	1	23	76
urinary tract	bladder carcinoma	0	4	9	0	6	90	0	3	0	2	0	3	0	0	6	6	0	9	138
upper aerodigestive	mouth	0	5	3	2	24	14	0	1	3	4	1	4	0	3	0	3	0	9	76
	Total	2	13	17	8	34	191	0	6	8	19	1	7	0	14	23	54	2	79	478

KRAS		codon 12: GGT						codon 13: GGC						codon 61: CAA						
		-C-	T--	-A-	C--	A--	-T-	-C-	T--	-A-	C--	A--	-T-	G--	--C/T	A--	-T-	-C-	-G-	
Primary tissue	cancer	12A	12C	12D	12R	12S	12V	13A	13C	13D	13R	13S	13V	61E	61H	61K	61L	61P	61R	Total
biliary tract	bile duct carcinoma	14	29	107	6	30	49	0	5	12	0	1	0	0	2	0	0	0	0	255
gall bladder	carcinoma	0	5	60	9	12	10	0	0	1	1	0	0	0	0	0	0	0	0	98
colorectal colon	adenocarcinoma	107	184	635	18	133	364	0	10	338	6	3	3	0	5	1	4	0	1	1812
	rectal adenocarcinoma	37	45	178	4	33	124	0	6	88	4	0	3	0	5	0	3	0	2	532
endometrium	carcinoma	39	26	121	3	12	68	2	4	26	0	1	1	0	3	0	0	0	0	306
H/L	haematopoietic neoplasm	8	4	38	2	10	12	0	0	25	0	0	0	0	4	1	2	0	0	106
	lymphoid neoplasm	19	7	43	4	10	10	0	0	48	0	1	0	0	3	0	0	3	0	148
lung	adenocarcinoma	106	545	222	27	59	279	1	43	31	1	1	1	0	11	1	5	0	2	1335
bronchioloalveolar	adenocarcinoma	6	42	38	3	4	33	0	2	0	0	0	0	0	0	0	0	0	0	128

HRAS		codon 12: GGC						codon 13: GGT							codon 61: CAG					
		-C-	T--	-A-	C--	A--	-T-	-C-	T--	-A-	C--	A--	-T-	G--	--C/T	A--	-T-	-C-	-G-	
Primary tissue	cancer	12A	12C	12D	12R	12S	12V	13A	13C	13D	13R	13S	13V	61E	61H	61K	61L	61P	61R	Total
	non small cell carcinoma	34	283	113	14	30	112	0	23	20	1	1	1	1	6	4	1	1	5	650
	squamous cell carcinoma	3	25	26	5	6	10	0	0	1	0	1	0	3	0	1	0	1	2	84
ovary	carcinoma	25	20	171	12	3	150	4	4	17	0	0	3	0	1	0	0	0	0	410
pancreas	ductal carcinoma	57	79	1312	312	67	812	0	1	13	0	2	0	0	6	0	0	0	0	2661
	PanIN	0	3	10	1	0	12	0	0	0	0	0	0	0	0	0	0	0	0	26
	acinar-ductal metaplasia	0	0	6	0	0	7	0	0	0	0	0	0	0	0	0	0	0	0	13
	adenoma	6	3	44	13	1	16	0	0	1	0	0	1	0	0	0	0	0	0	85
	autoimmune pancreatitis	0	0	10	0	0	0	0	0	0	0	0	0	0	0	0	0	0	0	10
	borderline tumour	0	2	11	2	0	6	0	0	1	0	0	0	0	0	0	0	0	0	22
	chronic pancreatitis	0	6	42	8	5	21	0	0	0	0	0	0	0	0	0	0	0	0	82
	dysplasia-in situ neoplasm	1	0	24	16	4	17	0	0	1	0	0	0	0	3	0	0	0	0	66
	hyperplasia	0	7	32	18	4	16	0	1	0	0	0	0	0	3	0	0	0	0	81
prostate	adenocarcinoma	0	9	13	1	2	35	0	0	15	0	6	0	0	0	2	0	0	1	84
skin	carcinoma	0	2	1	0	1	5	0	0	0	0	0	0	0	1	0	1	0	0	11
	malignant melanoma	0	0	3	2	1	8	0	0	1	0	0	0	0	1	0	3	0	1	20
small intestine	adenocarcinoma	4	8	25	0	4	10	0	0	2	0	0	1	0	1	0	0	0	0	55
stomach	adenocarcinoma	20	8	63	1	8	22	0	3	20	0	11	1	0	0	1	1	0	2	161
thyroid	carcinoma	5	18	35	4	15	8	1	1	22	2	10	0	0	0	1	0	3	4	129
urinary tract	bladder carcinoma	4	4	4	2	4	3	0	0	3	1	0	0	1	1	0	0	0	0	27
upper aerodigestive	mouth	1	3	3	1	6	0	0	0	0	0	1	0	0	0	0	0	0	1	16
	Total	496	1367	3390	488	464	2219	8	103	686	16	39	15	5	56	12	20	8	21	9413

NRAS		codon 12: GGT						codon 13: GGT							codon 61: CAA					
		-C-	T--	-A-	C--	A--	-T-	-C-	T--	-A-	C--	A--	-T-	G--	--C/T	A--	-T-	-C-	-G-	
Primary tissue	cancer	12A	12C	12D	12R	12S	12V	13A	13C	13D	13R	13S	13V	61E	61H	61K	61L	61P	61R	Total
H/L	haematopoietic neoplasm	22	32	185	8	56	31	12	14	93	29	3	29	2	28	24	20	6	29	623
	lymphoid neoplasm	7	11	60	0	17	11	1	4	54	7	1	6	1	21	37	20	11	27	296
skin	benign melanocytic nevus	0	2	4	0	0	0	0	0	0	1	1	0	0	0	55	1	0	35	99
	carcinoma	0	0	5	0	0	0	0	0	1	0	0	1	0	3	0	0	0	0	10

Cancer Res. Author manuscript; available in PMC 2012 November 15.

HRAS		codon 12: GGC						codon 13: GGT						codon 61: CAG					
		-C-	T--	-A-	C--	A--	-T-	-C-	T--	-A-	C--	A--	-T-	G--	--C/T	A--	-T-	-C-	-G-	
Primary tissue	cancer	12A	12C	12D	12R	12S	12V	13A	13C	13D	13R	13S	13V	61E	61H	61K	61L	61P	61R	Total
	malignant melanoma	2	2	28	5	8	2	1	0	14	12	0	16	1	24	273	64	2	301	755
thyroid	adenoma-nodule-goitre	0	1	0	0	0	2	0	1	0	0	0	0	1	1	12	1	0	44	63
	carcinoma	0	7	2	0	0	0	1	1	1	0	0	0	0	5	32	9	0	182	240
upper aerodigestive	larynx	0	0	0	0	20	0	0	0	0	0	0	0	0	0	0	0	0	0	20
	Total	31	55	284	13	101	46	15	20	163	49	5	52	5	82	433	115	19	618	2106